

Estimating the Geometric Error of Finite Volume Schemes for Conservation Laws on Surfaces for Generic Numerical Flux Functions

Jan Giesselmann and Thomas Müller

Abstract This contribution is concerned with finite volume schemes approximating scalar hyperbolic conservation laws on evolving hypersurfaces of \mathbb{R}^3 . Theoretical schemes assuming knowledge of all geometric quantities are compared to (practical) schemes defined on moving polyhedra approximating the surface. For the former schemes error estimates have already been proven, but the implementation of such schemes is not feasible for complex geometries. The latter schemes, in contrast, only require (easily) computable geometric quantities and are thus more useful for practical computations. In (Giesselmann and Müller *Number. Math.* 2014, doi:10.1007/s00211-014-0621-5) an estimate for the difference between solutions of both classes of schemes is proven. This estimate relies on an estimate for the geometric error of the numerical fluxes, which will be investigated in more detail in this contribution.

1 Introduction

Hyperbolic conservation laws serve as models for a wide variety of applications in continuum dynamics. In many applications the problems are posed on (moving) hypersurfaces. Examples include geophysical flows [16], transport processes on cell surfaces [14], surfactant flow on interfaces in multiphase flow [3] and petrol flow on a time dependent water surface. The numerical approximation of such problems was investigated by many groups in recent years, the shallow water equations on a rotating

J. Giesselmann

Institute for Applied Analysis and Numerical Simulation, University of Stuttgart,
Pfaffenwaldring 57, 70569 Stuttgart, Germany
e-mail: jan.giesselmann@mathematik.uni-stuttgart.de

T. Müller (✉)

Abteilung für Angewandte Mathematik, Universität Freiburg,
Hermann-Herder-Street 10, 79104 Freiburg, Germany
e-mail: mueller@mathematik.uni-freiburg.de

sphere for example were simulated in [4, 10, 15]. As we are interested in numerical analysis we restrict ourselves to the scalar case as a model problem. Well-posedness analysis can be found in [2, 6, 12] and the convergence of appropriate finite volume schemes was investigated in [1, 7, 9, 11].

The hitherto error analysis studied schemes defined on the curved surface assuming exact knowledge of all geometric quantities, e.g. areas and conormals. For engineering applications posed on hypersurfaces of \mathbb{R}^3 the geometric quantities are usually not known exactly but need to be approximated. In particular for moving surfaces for which the geometric quantities need to be computed in each time step it is desirable to reduce the computational effort needed to compute the geometric quantities.

In this situation it is important to know to which extent an approximation of the geometry influences the order of convergence.

We consider the following initial value problem, posed on a family of closed, smooth hypersurfaces $\Gamma = \Gamma(t) \subset \mathbb{R}^3$. For a derivation cf. e.g. [6]. For some $T > 0$, find $u : G_T := \bigcup_{t \in [0, T]} \Gamma(t) \times \{t\} \rightarrow \mathbb{R}$ with

$$\dot{u} + u \nabla_\Gamma \cdot v + \nabla_\Gamma \cdot f(u, \cdot, \cdot) = 0 \quad \text{in } G_T, \quad (1)$$

$$u(\cdot, 0) = u_0 \quad \text{on } \Gamma(0), \quad (2)$$

where v is the velocity of the material points of the surface and $u_0 : \Gamma(0) \rightarrow \mathbb{R}$ are initial data. For every $\bar{u} \in \mathbb{R}$, $t \in [0, T]$ the flux $f(\bar{u}, \cdot, t)$ is a smooth vector field tangential to $\Gamma(t)$, which depends Lipschitz on \bar{u} and smoothly on t . We impose the following growth condition

$$|\nabla_\Gamma \cdot f(\bar{u}, x, t)| \leq c + c|\bar{u}| \quad \forall \bar{u} \in \mathbb{R}, (x, t) \in G_T \quad (3)$$

for some constant $c > 0$. By \dot{u} we denote the material derivative of u , given by

$$\dot{u}(\Phi_t(x), t) := \frac{d}{dt} u(\Phi_t(x), t),$$

where $\Phi_t : \Gamma(0) \rightarrow \Gamma(t)$ is a family of diffeomorphisms depending smoothly on t , such that Φ_0 is the identity on $\Gamma(0)$. Obviously this excludes changes of the topology of Γ . We will assume that the movement of the surface and also the family Φ_t is prescribed. In [8] two approximations of u are considered. They are called the flat approximate and the curved approximate solution, respectively. The curved approximate solution is determined by a finite volume scheme defined on the curved surface, while the flat approximate solution is determined by a finite volume scheme defined on a polyhedron approximating the surface. We will explain these definitions in more detail in Sect. 2. In [8] an estimate for the difference of the curved and the flat approximate solution was obtained. For completeness we will state it as Theorem 1. In [8] it turned out that while the numerical fluxes of the curved scheme need to satisfy the classical consistency, conservation and monotonicity conditions, the fluxes of the flat scheme need to satisfy a geometric error estimate, cf. (9). The main contribution

of this work is a rather generic framework showing that standard numerical fluxes satisfy this condition in Sect. 4.

2 The Finite Volume Schemes

For our analysis the family of triangulations $\mathcal{T}_h(t)$ of the surfaces needs to be suitably linked to polyhedral approximations $\Gamma_h(t)$ of the surfaces.

The triangulation and the definition of the finite volume scheme on Γ_h are in the same spirit as the one in [13], developed for the diffusion equation on evolving surfaces. They are detailed in [8]. Let us simply mention that a triangulation $\tilde{\mathcal{T}}_h(t)$ of the polyhedral $\Gamma_h(t)$ is given by its decomposition into faces. Note that in what follows we will consider all faces and edges to be closed sets. We define the triangulation $\mathcal{T}_h(t)$ on $\Gamma(t)$ as the image of $\tilde{\mathcal{T}}_h(t)$ under a projection in normal direction from $\Gamma_h(t)$ to $\Gamma(t)$. We denote curved cells with $K(t)$ and the curved faces with $e(t)$. A flat quantity corresponding to some curved quantity is denoted by the same letter and a bar, e.g. let $K(t) \subset \Gamma(t)$ be a curved cell then $\bar{K}(t)$ is the corresponding flat cell. In order to reflect the fact that all triangulations share the same grid topology we introduce the following notation. We denote by K the family of all curved triangles relating to the same triangle $\bar{K}(0)$ on $\Gamma_h(0)$. We do the same for e, \bar{K}, \bar{e} . Analogously by \mathcal{T}_h we denote the family of such families of triangles K .

We will use the following notation. By $h_{K(t)} := \text{diam}(K(t))$ we denote the diameter of each cell, furthermore $h := \max_{t \in [0, T]} \max_{K(t)} h_{K(t)}$ and $|K(t)|, |\partial K(t)|$ are the Hausdorff measures of $K(t)$ and the boundary of $K(t)$ respectively. When we write $e(t) \subset \partial K(t)$ we mean $e(t)$ to be a face of $K(t)$.

In addition, we need to impose the following assumption uniformly on all flat triangulations $\tilde{\mathcal{T}}_h(t)$. There is a constant number $\alpha > 0$ such that for each flat cell $\bar{K}(t) \in \tilde{\mathcal{T}}_h(t)$ we have

$$\alpha h^2 \leq |\bar{K}(t)| \quad \text{and} \quad \alpha |\partial \bar{K}(t)| \leq h. \tag{4}$$

In [8] it was shown that this implies the respective estimate for the curved triangulation.

2.1 The Finite Volume Scheme on Curved Elements

Let us briefly review the notion of finite volume schemes on moving curved surfaces. We consider a sequence of times $0 = t_0 < t_1 < t_2 < \dots$ and set $I_n := [t_n, t_{n+1}]$. We assign to each $n \in \mathbb{N}$ and $K \in \mathcal{T}_h$ the term u_K^n approximating the mean value of u on $\bigcup_{t \in I_n} K(t) \times \{t\}$ and to each $K \in \mathcal{T}_h$ and face $e \subset \partial K$ a numerical flux function $f_{K,e}^n : \mathbb{R}^2 \rightarrow \mathbb{R}$, which should approximate

$$\frac{1}{|I_n| |e(t_n)|} \int_{I_n} \int_{e(t)} \langle f(u(x, t), x, t), \mu_{K(t), e(t)}(x) \rangle de(t) dt, \tag{5}$$

where $de(t)$ is the line element, $\mu_{K(t), e(t)}(x)$ is the unit conormal to $e(t)$ pointing outwards from $K(t)$ and $\langle \cdot, \cdot \rangle$ is the standard Euclidean inner product. Please note that $\mu_{K(t), e(t)}(x)$ is tangential to $\Gamma(t)$. Then the ‘‘curved’’ finite volume scheme is given by

$$\begin{aligned} u_K^0 &:= \int_{K(0)} u_0(x) d\Gamma(0), \\ u_K^{n+1} &:= \frac{|K(t_n)|}{|K(t_{n+1})|} u_K^n - \frac{|I_n|}{|K(t_{n+1})|} \sum_{e \subset \partial K} |e(t_n)| f_{K,e}^n(u_K^n, u_{K_e}^n), \\ u^h(x, t) &:= u_K^n \quad \text{for } t \in [t_n, t_{n+1}), x \in K(t), \end{aligned} \tag{6}$$

where K_e denotes the cell sharing face e with K and $d\Gamma(0)$ is the surface element. We assume the numerical fluxes to be consistent, conservative, monotone, and uniformly Lipschitz continuous, which is standard in the error analysis of the curved schemes. Let L denote the Lipschitz constant of the numerical fluxes, then additionally the CFL condition

$$t_{n+1} - t_n \leq \frac{\alpha^2 h}{8L} \tag{7}$$

has to be imposed to ensure stability. Note, that the right hand side of (7) is related to the minimal diameter of inner circles of cells through the constant α^2 .

2.2 The Finite Volume Scheme on Flat Elements

In this section we define finite volume schemes on $\bar{\mathcal{T}}_h$ which are in the spirit of (6) but only rely on easily accessible geometrical information. We like to point out that the calculation of areas and lengths is straightforward for flat elements. As well, the approximation of integrals can be achieved using quadrature formulas by mapping cells and edges to a standard triangle and the unit interval, respectively, using affine linear maps. In this fashion we obtain for every time $t \in [0, T]$ quadrature operators $Q_{\bar{K}(t)}$ on flat cells and $Q_{\bar{e}(t)}$ on flat edges of order $p_1, p_2 \geq 1$, respectively. In addition for any compact interval $I \subset [0, T]$ the term Q_I denotes a quadrature operator of order $p_3 \geq 1$ on I . For Lipschitz continuous numerical flux functions $f_{K,\bar{e}}^n : \mathbb{R} \times \mathbb{R} \rightarrow \mathbb{R}$ we define the finite volume scheme on flat elements by

$$\begin{aligned} \bar{u}_{\bar{K}}^0 &:= \frac{1}{|\bar{K}(0)|} Q_{\bar{K}(0)}(u_0(a(\cdot, 0))), \\ \bar{u}_{\bar{K}}^{n+1} &:= \frac{|\bar{K}(t_n)|}{|\bar{K}(t_{n+1})|} \bar{u}_{\bar{K}}^n - \frac{|I_n|}{|\bar{K}(t_{n+1})|} \sum_{\bar{e} \subset \partial \bar{K}} |\bar{e}(t_n)| \bar{f}_{\bar{K}, \bar{e}}^n(\bar{u}_{\bar{K}}^n, \bar{u}_{\bar{K}, \bar{e}}^n), \\ \bar{u}^h(x, t) &:= \bar{u}_{\bar{K}}^n, \quad \text{for } t \in [t_n, t_{n+1}), x \in K(t), \end{aligned} \tag{8}$$

where a in (8)₁ is the projection map in normal direction from Γ_h to Γ , see [5, e.g.]. Note that by (8)₃ the function \bar{u}^h is defined on G_T . For the numerical analysis in [8] the following estimate for the (geometric) error between the numerical fluxes $f_{K,e}^n$ and $\bar{f}_{\bar{K}, \bar{e}}^n$ is crucial:

$$\left| f_{K,e}^n(u, v) - \bar{f}_{\bar{K}, \bar{e}}^n(u, v) \right| \leq Ch^2 \quad \forall (u, v) \in \mathcal{K}, K \in \mathcal{T}_h, e \subset \partial K, \tag{9}$$

where \mathcal{K} is a compact subset of \mathbb{R}^2 and C a constant depending only on G_T , f and \mathcal{K} . In particular, C depends on the curvature of the surface, which is bounded, as we consider closed surfaces and finite times. The dependence on the curvature is rather complex and is related to the approximation of all geometric quantities, see [8, Lemma 2, 3 and 4] for details. The compact set \mathcal{K} is due to L^∞ -estimates for the finite volume schemes, cf. [8, Lemma 7 and 9], and allows the control of f and its derivatives. It was shown in [8] that (9) holds for the Lax-Friedrichs flux, in case the flat and the curved scheme use the same amount of numerical viscosity.

3 Error Estimate

The main upshot of [8] is the following theorem.

Theorem 1 *For initial data $u_0 \in L^\infty(\Gamma(0))$, let u^h denote the solution of the curved finite volume scheme (6) and let \bar{u}^h denote the solution of the flat finite volume scheme (8). Let the quadrature operators $Q_{\bar{K}}(0)$ and the initial data u_0 be such that*

$$\|u^h(0) - \bar{u}^h(0)\|_{L^1(\Gamma(0))} \leq Ch \tag{10}$$

for some constant C . Let the curved numerical flux functions be consistent, conservative and monotone and let the time step satisfy (7). Let, additionally, (9) hold for the flat numerical flux functions. Then, for fixed $T > 0$, the difference between u^h and \bar{u}^h satisfies

$$\|u^h(T) - \bar{u}^h(T)\|_{L^1(\Gamma(T))} \leq Ch, \tag{11}$$

for some constant C depending on G_T , f , u_0 .

Remark 1 Note that the arising geometry errors can be neglected compared to the error between the curved approximate solution and the exact solution, i.e. both

approximate solutions converge to the entropy solution with the same convergence rate $\mathcal{O}(h^{1/4})$, see [9, 11]. Numerical examples in [8] show that the proven convergence rate (11) is optimal under the assumptions for the numerical analysis. However, for most numerical experiments higher orders of convergence are observed.

The analysis indicates that the geometry error poses an obstacle to the construction of higher order schemes. Numerical experiments in [8] show that this is indeed the case. Therefore, to obtain higher order convergence, also the geometry of the curved surface has to be approximated sufficiently accurate. One could think of extending this work to the case of higher order schemes, Discontinuous Galerkin or higher order finite volume schemes e.g., defined on higher order approximations of the moving surface.

In what follows we will present a generic framework to investigate whether flux functions satisfy (9).

4 Determining Which Numerical Fluxes Satisfy (9)

In order to construct numerical fluxes for the curved scheme from standard numerical flux functions, originally developed for equations posed in \mathbb{R} , we define, for every $n \in \mathbb{N}$, $K \in \mathcal{T}_h$, $e \in \partial K$, the function

$$c_{K,e}^n(u) := \frac{1}{|I_n| |e(t_n)|} \int_{I_n} \int_{e(t)} \langle f(u, x, t), \mu_{K(t),e(t)}(x) \rangle de(t) dt \quad \forall u \in \mathbb{R},$$

that can be interpreted as an approximation of the flux across the edge e during the time interval I_n .

For a function $\tilde{f} : \mathbb{R} \rightarrow \mathbb{R}$, let $G[\tilde{f}] : \mathbb{R} \times \mathbb{R} \rightarrow \mathbb{R}$ be a one-dimensional numerical flux function that is consistent with \tilde{f} , monotone, conservative, i.e.

$$G[\tilde{f}](u, v) = -G[-\tilde{f}](v, u) \quad \forall u, v \in \mathbb{R},$$

and Lipschitz-continuous. From $G : C^1(\mathbb{R}) \rightarrow C^1(\mathbb{R}^2)$ we derive a generic family of corresponding numerical flux functions

$$f_{K,e}^n(u, v) := G[c_{K,e}^n](u, v) \quad \text{for all } u, v \in \mathbb{R} \tag{12}$$

for the curved scheme. Note that monotonicity, conservation, Lipschitz-continuity and consistency for the surface numerical fluxes are inherited from the 1-D numerical fluxes. The Lax-Friedrichs flux from [8] for the curved scheme on moving surfaces can be recovered by ${}^{\text{LF}}f_{K,e}^n(u, v) = {}^{\text{LF}}G[c_{K,e}^n](u, v)$ with the one-dimensional Lax-Friedrichs flux

$${}^{\text{LF}}G[\tilde{f}](u, v) := \frac{1}{2} \left(\tilde{f}(u) + \tilde{f}(v) \right) + \lambda(u - v),$$

for a sufficiently large diffusion coefficient $\lambda \geq 0$. The flat scheme from [8] can be recovered by replacing $c_{K,e}^n$ accordingly, i.e.

$$\text{LF } \tilde{f}_{\bar{K},\bar{e}}^n(u, v) = \text{LF } G[\tilde{c}_{\bar{K},\bar{e}}^n](u, v)$$

with

$$\tilde{c}_{\bar{K},\bar{e}}^n(u) := \frac{1}{|I_n|} Q_{I_n} \left[\frac{1}{|\bar{e}(t_n)|} Q_{\bar{e}(\cdot)} \left(\langle f(u, \cdot, \cdot), \bar{\mu}_{\bar{K}(\cdot),\bar{e}(\cdot)} \rangle \right) \right].$$

In this manner we can also construct Godunov numerical fluxes on moving surfaces with the help of the one-dimensional Godunov numerical flux functions

$$\text{GV } G[\tilde{f}](u, v) := \begin{cases} \min_{w \in I(u,v)} \tilde{f}(w) & \text{if } u \leq v, \\ \max_{w \in I(u,v)} \tilde{f}(w) & \text{if } v \leq u. \end{cases}$$

In order to show that (9) holds for the (geometric) error between flat and curved numerical fluxes that are based on the same one-dimensional flux functions, we recall from [8, Proof of Lemma 5] that for every compact $\mathcal{K} \subset \mathbb{R}$ there exists $c = c(\mathcal{K}) > 0$ such that

$$|c_{K,e}^n(u) - \tilde{c}_{\bar{K},\bar{e}}^n(u)| = |E_{K,e}^n(u)| \leq ch^2 \quad \forall u \in \mathcal{K}. \tag{13}$$

This estimate at hand it is an easy exercise to show that both, the Lax-Friedrichs and the Godunov scheme satisfy (9), as for any compact $\mathcal{K} \subset \mathbb{R}$

$$\|{}^i G[\tilde{f}_1] - {}^i G[\tilde{f}_2]\|_{L^\infty(\mathcal{K}^2)} \leq \|\tilde{f}_1 - \tilde{f}_2\|_{L^\infty(\mathcal{K})} \quad i = \text{LF, GV}. \tag{14}$$

For the Engquist-Osher flux the situation is slightly different. However, it can be shown analogously to the derivation of (13) that

$$\left| \frac{d c_{K,e}^n}{d u}(u) - \frac{d \tilde{c}_{\bar{K},\bar{e}}^n}{d u}(u) \right| \leq ch^2. \tag{15}$$

Moreover, the Engquist-Osher numerical flux operator

$$\text{EO } G[\tilde{f}](u, v) = \tilde{f}(0) + \int_0^u \max\{\tilde{f}'(s), 0\} ds + \int_0^v \min\{\tilde{f}'(s), 0\} ds$$

satisfies

$$\|\text{EO } G[\tilde{f}_1] - \text{EO } G[\tilde{f}_2]\|_{L^\infty(\mathcal{K}^2)} \leq C(\mathcal{K}) \|\tilde{f}'_1 - \tilde{f}'_2\|_{L^\infty(\mathcal{K})} \tag{16}$$

for any compact $\mathcal{K} \subset \mathbb{R}$. Thus, the Engquist-Osher flux satisfies (9).

Acknowledgments We gratefully acknowledge that the work of T.M. was supported by the German Research Foundation (DFG) via SFB TR 71 ‘Geometric Partial Differential Equations’ and by the

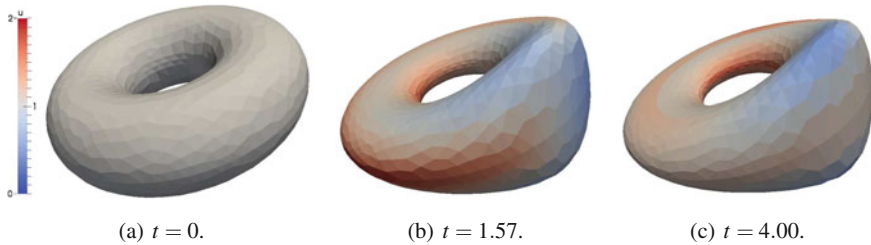


Fig. 1 Flat approximate solution for (1)–(2) at three different times with Godunov numerical flux functions for the following problem, which was originally studied in [8]: A deforming torus is considered as computational domain Γ and $T = 4$ as final time. Within the time interval $[0, 2]$ the *left half* of the torus undergoes compression whereas the *right half* is stretched, while $\Gamma(t)$ remains constant for $t \in [2, 4]$. A Burgers-type flux function $f = f(u, x) = \frac{1}{2}u^2(x_2, -x_1, 0)^T$ and constant initial values $u_0 \equiv 1$ are chosen. The time step size is chosen dynamically for each time step in order to guarantee stability. In spite of the constant initial values, a shock wave is induced due to the change of geometry (compression and rarefaction) and the nonlinearity of the flux function. Note that the actual computation was performed on a deforming polyhedron approximating the deforming torus. All simulations have been performed within the DUNE-FEM module using AluGrid as grid implementation. Confer [8] for implementation references and more detailed simulations

German National Academic Foundation. J.G. would like to thank the DFG for financial support of the project ‘Modeling and sharp interface limits of local and non-local generalized Navier–Stokes–Korteweg Systems’.

We would like to express our gratitude to the two anonymous referees of [8] whose constructive criticism initiated this work.

References

1. Amorim, P., Ben-Artzi, M., LeFloch, P.G.: Hyperbolic conservation laws on manifolds: total variation estimates and the finite volume method. *Methods Appl. Anal.* **12**(3), 291–323 (2005)
2. Ben-Artzi, M., LeFloch, P.G.: Well-posedness theory for geometry-compatible hyperbolic conservation laws on manifolds. *Ann. Inst. H. Poincaré Anal. Non Linéaire* **24**(6), 989–1008 (2007)
3. Bothe, D., Prüss, J., Simonett, G.: Well-posedness of a two-phase flow with soluble surfactant. In: *Nonlinear Elliptic and Parabolic Problems, Programming Nonlinear Differential Equations Applications*, vol. 64, pp. 37–61. Birkhäuser, Basel (2005)
4. Calhoun, D.A., Helzel, C., LeVeque, R.J.: Logically rectangular grids and finite volume methods for PDEs in circular and spherical domains. *SIAM Rev.* **50**(4), 723–752 (2008)
5. Dziuk, G., Elliott, C.M.: Finite elements on evolving surfaces. *IMA J. Numer. Anal.* **27**(2), 262–292 (2007)
6. Dziuk, G., Kröner, D., Müller, T.: Scalar conservation laws on moving hypersurfaces. *Interfaces Free Boundaries* **15**(2), 203–236 (2013)
7. Giesselmann, J.: A convergence result for finite volume schemes on Riemannian manifolds. *M2AN Math. Model. Numer. Anal.* **43**(5), 929–955 (2009)
8. Giesselmann, J., Müller, T.: Geometric error of finite volume schemes for conservation laws on evolving surfaces. *Numer. Math.* (2014). doi:[10.1007/s00211-014-0621-5](https://doi.org/10.1007/s00211-014-0621-5)

9. Giesselmann, J., Wiebe, M.: Finite volume schemes for balance laws on time-dependent surfaces. In: *Numerical Methods for Hyperbolic Equations*, pp. 251–258. CRC Press, London (2012)
10. Giraldo, F.X.: High-order triangle-based discontinuous galerkin methods for hyperbolic equations on a rotating sphere. *J. Comput. Phys.* **214**(2), 447–465 (2006)
11. LeFloch, P.G., Okutmustur, B., Neves, W.: Hyperbolic conservation laws on manifolds. An error estimate for finite volume schemes. *Acta Math. Sin. (Engl. Ser)* **25**(7), 1041–1066 (2009)
12. Lengeler, D., Müller, T.: Scalar conservation laws on constant and time-dependent riemannian manifolds. *J. Differ. Equ.* **254**(4), 1705–1727 (2013)
13. Lenz, M., Nemađjieu, S.F., Rumpf, M.: A convergent finite volume scheme for diffusion on evolving surfaces. *SIAM J. Numer. Anal.* **49**(1), 15–37 (2011)
14. Reister, E., Seifert, U.: Lateral diffusion of a protein on a fluctuating membrane. *EPL (Europhysics Letters)* **71**(5), 859 (2005)
15. Rossmannith, J.A.: A wave propagation algorithm for hyperbolic systems on the sphere. *J. Comput. Phys.* **213**(2), 629–658 (2006)
16. Williamson, D.L., Drake, J.B., Hack, J.J., Jakob, R., Swarztrauber, P.N.: A standard test set for numerical approximations to the shallow water equations in spherical geometry. *J. Comput. Phys.* **102**(1), 211–224 (1992)